SANDIA REPORT

SAND2011-1767
Unlimited Release
Printed April 2011

GMTI Radar Minimum Detectable Velocity

John A. Richards

Prepared by
Sandia National Laboratories
Albuquerque, New Mexico 87185 and Livermore, California 94550

Sandia National Laboratories is a multi-program laboratory managed and operated by Sandia Corporation, a wholly owned subsidiary of Lockheed Martin Corporation, for the U.S. Department of Energy's National Nuclear Security Administration under contract DE-AC04-94AL85000.

Sandia National Laboratories

Issued by Sandia National Laboratories, operated for the United States Department of Energy by Sandia Corporation.

Printed in the United States of America. This report has been reproduced directly from the best available copy.

Available to DOE and DOE contractors from
U.S. Department of Energy
Office of Scientific and Technical Information
P.O. Box 62
Oak Ridge, TN 37831

Telephone: (865) 576-8401
Facsimile: (865) 576-5728
E-Mail: reports@adonis.osti.gov
Online ordering: http://www.osti.gov/bridge

Available to the public from
U.S. Department of Commerce
National Technical Information Service
5285 Port Royal Rd
Springfield, VA 22161

Telephone: (800) 553-6847
Facsimile: (703) 605-6900
E-Mail: orders@ntis.fedworld.gov
Online ordering: http://www.ntis.gov/help/ordermethods.asp?loc=7-4-0#online

SAND2011-1767
Unlimited Release
Printed April 2011

GMTI Radar Minimum Detectable Velocity

John A. Richards
Sensor Exploitation Applications Department
Sandia National Laboratories
P.O. Box 5800
Albuquerque, NM 87185-1163

Abstract

Minimum detectable velocity (MDV) is a fundamental consideration for the design, implementation, and exploitation of ground moving-target indication (GMTI) radar imaging modes. All single-phase-center air-to-ground radars are characterized by an MDV, or a minimum radial velocity below which motion of a discrete nonstationary target is indistinguishable from the relative motion between the platform and the ground. Targets with radial velocities less than MDV are typically overwhelmed by endoclutter ground returns, and are thus not generally detectable. Targets with radial velocities greater than MDV typically produce distinct returns falling outside of the endoclutter ground returns, and are thus generally discernible using straightforward detection algorithms. This document provides a straightforward derivation of MDV for an air-to-ground single-phase-center GMTI radar operating in an arbitrary geometry.

Acknowledgment

This work was funded by the United States Air Force Electronic Systems Center.

Contents

Figures

1 GMTI Overview

Ground moving-target indication (GMTI) radar imaging modes enable the remote detection and characterization of nonstationary objects [3, 2, 1]. GMTI data is derived from range-Doppler maps of the imaged scene, in which reflectivity is measured as a function of range r and range rate dr/dt (i.e., the radial velocity of an imaged object with respect to the radar platform). All single-phase-center radar air-to-ground GMTI modes are characterized by a minimum detectable velocity (MDV)—more precisely, a minimum detectable *radial* velocity, or a minimum detectable range rate—below which motion of a discrete nonstationary target is indistinguishable from the relative motion between the platform and the ground. Targets with radial velocities less than MDV are typically overwhelmed by endoclutter ground returns, and are thus not generally detectable. The MDV for a particular radar imaging scenario is a function of numerous parameters, including:

- Platform velocity v, relative to the ground;
- Platform altitude h, relative to the ground at scene center;
- Antenna elevation two-sided beamwidth β_e;
- Antenna azimuth two-sided beamwidth β_a;
- Imaging depression angle θ to scene center;
- Imaging squint angle ψ (where $\psi = 0^\circ$ indicates a directly forward-looking geometry);
- Slant-plane range-bin spacing δ_r;
- Number of range bins in the image N_r.

These parameters impact MDV because they dictate the extent of the imaged scene on the ground and the relative motion of different ground points across that extent, as described shortly. The collective set of all imaged ground points comprises the endoclutter.

Figure 1 depicts an arbitrary imaging geometry involving level platform motion over level ground. This imaging geometry is completely characterized by the angles θ and ψ, the platform height h, and the platform velocity v. The scene center is taken to be the ground location pointed at by the sensor boresight. The scene center has a slant range of

$$r_0 = \frac{h}{\sin\theta} \tag{1}$$

a ground range of

$$\tilde{r}_0 = \frac{h}{\tan\theta}. \tag{2}$$

The scene extent is determined by the projection of the antenna mainlobe on the ground. The projection of the antenna mainlobe on the ground in any geometry is a teardrop-shaped region with major and minor axes dictated by β_e, β_a, and r_0. Not every point in the projected beam yields a return in a range-Doppler or GMTI image: the reflected energy is subjected to a range gate, indicated by the shaded region in Figure 1, that is typically taken to be symmetric about the scene center. The range gate has slant-plane extent of

$$\Delta_r = N_r\delta_r \tag{3}$$

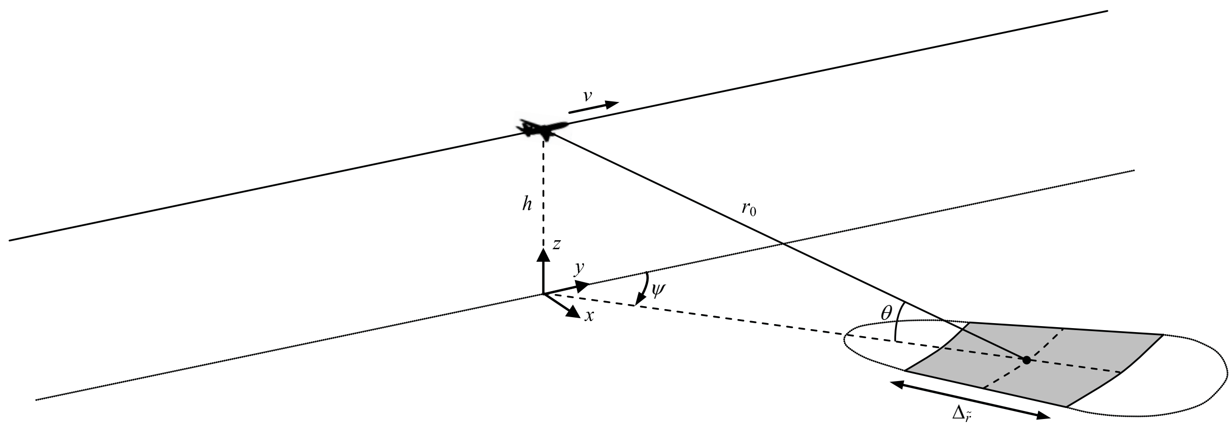

Figure 1. Arbitrary geometry. The shaded region is the range-gated, illuminated ground region that is used to form the range-Doppler image and the GMTI returns.

and ground-plane extent of

$$\Delta_{\tilde{r}} = \frac{N_r \delta_r}{\cos\theta}. \tag{4}$$

The range-gated portion of the ground projection of the antenna mainlobe is thus approximately an annular sector. Objects outside of this range gate will yield no range-Doppler or GMTI returns in the image products.[1]

Target velocity in GMTI radar imaging modes is usually measured with respect to the scene center. The scene center has a range rate that is dictated by the platform velocity and imaging geometry:

$$\frac{dr_0}{dt} = v\cos\theta\cos\psi. \tag{5}$$

Rather than measuring the absolute range rate dr/dt between the platform and imaged objects, GMTI modes measure a relative range rate dr'/dt with respect to the scene center:

$$\frac{dr'}{dt} = \frac{dr}{dt} - \frac{dr_0}{dt}. \tag{6}$$

Hence, a "zero-velocity" target is a target whose absolute radial velocity is identical to that of the stationary scene center. Note that a zero-velocity target may actually be nonstationary: it will have a radial range rate that is equal to that of the scene center, but it may have a large tangential velocity component. In general, a target moving at velocity v_t with respect to the scene center will have an apparent relative range rate of

$$\frac{dr'_t}{dt} = v_t\cos\theta_t\cos\phi_t, \tag{7}$$

where θ_t is the depression angle from the platform to the target, and ϕ_t is the angular deviation between the ground-projected platform-to-scene-center look vector and the target velocity vector.

[1] Note that for extremely coarse range-bin spacing δ_r or for extremely close imaging ranges, the apparent range extent may exceed the projected range beam extent. In such cases, the beam range extent, and not the range gate, will limit the imaged scene size.

Consideration of the GMTI imaging geometry of Figure 1 reveals that different points within the imaged scene have different, and nonzero, relative range rates dr'/dt. The collective radar energy reflected from the set of all imaged ground points, each with a particular range rate, produces the endoclutter response characteristic of single-phase-center radar air-to-ground range-Doppler images. The particular imaging geometry (that is, the precise choices of ψ, θ, h, and v) dictate the distribution of range rates within the imaged scene for that geometry, and thus determine the characteristics of the endoclutter response—including MDV—for that geometry. In Section 4 we derive an expression for MDV in an arbitrary imaging geometry, as depicted in Figure 1. First, however, we consider MDV for two common and illustrative image geometries: broadside-looking (presented in Section 2) and forward-looking (presented in Section 3).

2 Broadside-Looking Geometry

A pure broadside-looking imaging geometry, as depicted in Figure 2, is defined as any geometry in which squint angle ψ is 90° or 270°. It follows from (5) that the scene center in any broadside geometry has an absolute radial velocity of 0. However, any point in the leading direction of the projected beam—such as point A in Figure 2—has a negative instantaneous radial velocity, because the range between the platform and the point is decreasing. Similarly, any point in the trailing direction of the projected beam—such as point B in Figure 2—has a positive radial velocity. It can be shown that the relative range rate of a stationary object at point A is

$$\frac{dr'_A}{dt} = -v \sin\left(\frac{\beta_a}{2}\right) \tag{8}$$

and, likewise, the relative range rate of a stationary object at point B is

$$\frac{dr'_B}{dt} = v \sin\left(\frac{\beta_a}{2}\right). \tag{9}$$

Points A and B respectively attain approximately the minimum and maximum range rates of any illuminated, range-gated ground points in a broadside-looking geometry.[2] All imaged ground points (i.e., the entirety of the endoclutter) will thus have relative range rates between that specified in (8) and that specified in (9), depending on their relative position between points A and B. The implication is thus that the MDV in a broadside imaging mode is

$$\mathrm{MDV}_{\mathrm{brd}} = v \sin\left(\frac{\beta_a}{2}\right). \tag{10}$$

It is important to stress that this MDV is a minimum detectable *radial* velocity. A vehicle moving at a much greater absolute velocity, but with a *radial* velocity component—as in (7)—below the MDV specified in (10), will not be detectable.

Note that the broadside MDV of (10) is a function of only two parameters, the platform velocity and the azimuth beamwidth. It is independent of imaging range, platform altitude, elevation beamwidth, range gate extent, and all other parameters. Azimuth beamwidth, like other antenna parameters, is usually fixed by physical antenna characteristics. As such, any attempt to reduce broadside MDV of a single phase-center system will usually require a reduction in platform velocity.

[2] In fact, the points at the corners of the annular region depicted in Figure 2, located radially outward from A and B, actually achieve slightly more extreme range rates than do A and B. However, because the difference is negligible for most imaging geometries, and because the use of the alternate points complicates the derivation of MDV, most approaches follow from consideration of points A and B.

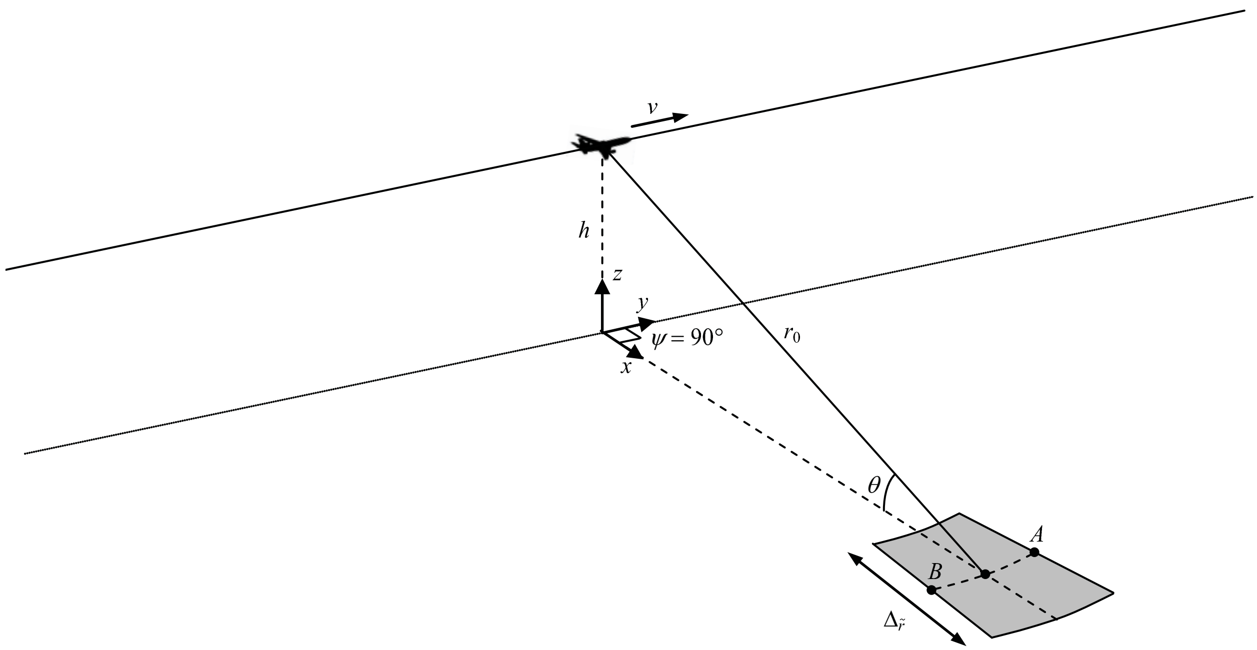

Figure 2. Broadside-looking geometry. The shaded region is the range-gated, illuminated ground region that is used to form the range-Doppler image and the GMTI returns. Point A represents the leading edge of the beam, which attains the greatest negative range rate; point B represents the trailing edge of the beam, which attains the greatest positive range rate.

3 Forward-Looking Geometry

A pure forward-looking imaging geometry, as depicted in Figure 3, is defined as a geometry in which squint angle ψ is $0°$. This leads to a different MDV than that obtained in a broadside imaging geometry. It follows from (5) that the scene center in a forward-looking geometry has a nonzero range rate of

$$\frac{dr_0}{dt} = v\cos\theta. \tag{11}$$

The trailing and leading edges of the range gate—represented in Figure 3 by points C and D, respectively—will have slightly different range rates than the scene center. Points C and D attain approximately the minimum and maximum range rates of any illuminated, range-gated ground points in a forward-looking geometry.[3] The ground range from the platform to point C is

$$\tilde{r}_C = \tilde{r}_0 - \frac{\Delta_{\tilde{r}}}{2}. \tag{12}$$

Similarly, the ground range from the platform to point D is

$$\tilde{r}_D = \tilde{r}_0 + \frac{\Delta_{\tilde{r}}}{2}. \tag{13}$$

These ground ranges can be used to calculate the depression angle to point C,

$$\theta_C = \tan^{-1}\left(\frac{h}{\tilde{r}_C}\right), \tag{14}$$

and the depression angle to point D,

$$\theta_D = \tan^{-1}\left(\frac{h}{\tilde{r}_D}\right). \tag{15}$$

It can be shown that the relative range rate of a stationary object at point C is

$$\frac{dr'_C}{dt} = v(\cos\theta_C - \cos\theta) \tag{16}$$

and, likewise, the relative range rate of a stationary object at point D is

$$\frac{dr'_D}{dt} = v(\cos\theta_D - \cos\theta). \tag{17}$$

For any reasonable imaging scenario, we will have

$$0° < \theta_D < \theta < \theta_C < 90°, \tag{18}$$

and thus the relative range rate of (16) will be negative and the relative range rate of (17) will be positive. Furthermore, the magnitude of (17) will be greater than that of (16). Hence, in a forward-looking geometry, the MDV may be taken as

$$\mathrm{MDV}_{\mathrm{fwd}} = v(\cos\theta_D - \cos\theta). \tag{19}$$

[3] In fact, the points at the corners of the trailing edge, located circumferentially leftward and rightward from C, actually achieve slightly smaller range rates than does C. As in the previous section, however, the difference is negligible for most imaging geometries, and use of point C simplifies the ensuing derivation.

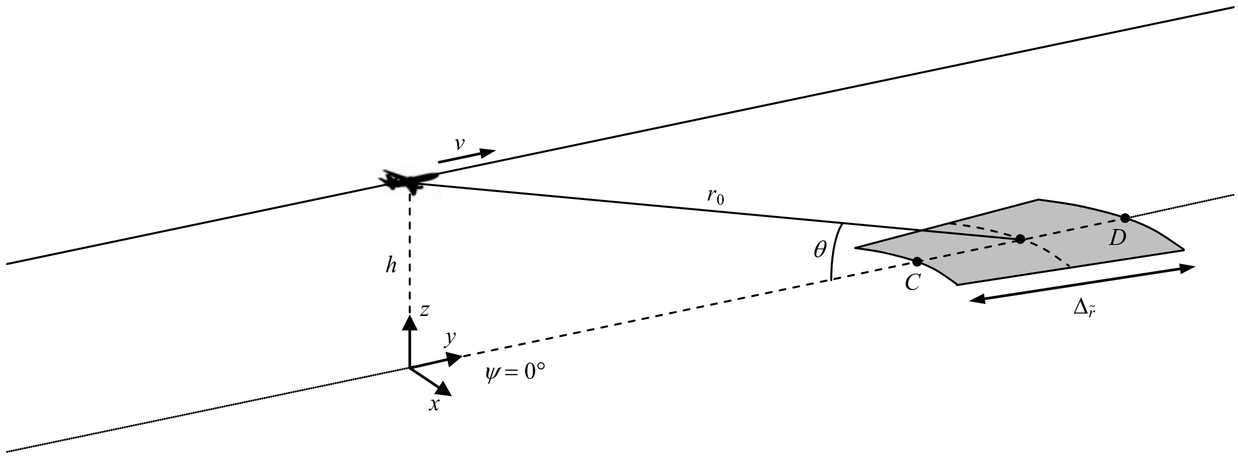

Figure 3. Forward-looking geometry. The shaded region is the range-gated, illuminated ground region that is used to form the range-Doppler image and the GMTI returns. Point C represents the trailing edge of the range gate, which attains the greatest negative relative range rate (with respect to the scene center); point D represents the leading edge of the range gate, which attains the greatest positive relative range rate (with respect to the scene center).

This can be re-expressed in terms of other parameters as

$$\mathrm{MDV}_{\mathrm{fwd}} = v \left(\frac{\tilde{r}_0 + \frac{\Delta_{\tilde{r}}}{2}}{\left(h^2 + \left(\tilde{r}_0 + \frac{\Delta_{\tilde{r}}}{2}\right)^2\right)^{1/2}} - \cos\theta \right). \tag{20}$$

As previously, it is important to stress that this MDV is a minimum detectable *radial* velocity. A vehicle moving at a much greater absolute velocity, but with a *radial* velocity component—as in (7)—below this MDV, will not be detectable.

Comparing (10) and (19), it is clear that the forward-looking MDV is fundamentally different from the broadside MDV. In a broadside imaging geometry, MDV depends only on azimuth beamwidth and platform velocity. In a forward-looking geometry, MDV depends on platform velocity and range gate extent. As in the broadside-looking case, there are limited options available for reducing MDV in the forward-looking geometry. Platform altitude, ground range, and imaging depression are usually constrained by operational requirements; range gate extent (i.e., range-bin spacing and number of range bins in the image) is usually dictated by the application at hand. As such, the most practical way to reduce MDV in a forward-looking geometry is usually to reduce platform velocity v. This is exactly analogous to the broadside-looking situation.

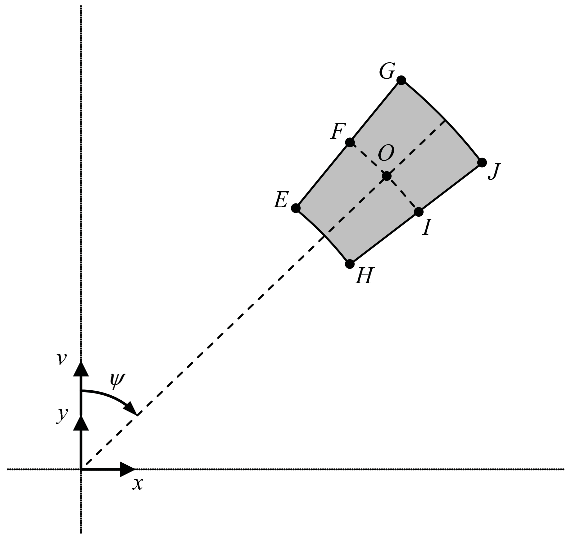

Figure 4. Imaged ground region in arbitrary geometry. The shaded region is the range-gated, illuminated ground region that is used to form the range-Doppler image and the GMTI returns. For most geometries with $0° \leq \psi \leq 90°$, point G will achieve the maximum relative range rate with respect to point O, and point H will achieve the minimum relative range rate with respect to point O. The depicted coordinate axes are located at the ground-projected location of the imaging platform, with y-axis oriented along the direction of platform motion and x-axis oriented orthogonally within the ground plane.

4 Arbitrary Geometry

The geometries considered in the previous two sections—broadside-looking and forward-looking—represent two particular choices of squint angle ψ (namely, 90° and 0°). In this section we turn our attention to MDV for the arbitrary geometry depicted in Figure 1, in which ψ may take on any value between 0° and 90°.[4] Figure 4 presents a more detailed illustration of the range-gated, illuminated ground region in an arbitrary imaging geometry. This region has scene center O, and is delineated by boundary points E, F, G, H, I, and J. Points F, O, and I are all at ground range $\tilde{r}_0$ from the sensor. Points E and H are located at the near end of the range gate, at ground range $\tilde{r}_0 - \Delta_{\tilde{r}}/2$; points G and J are located at the far end of the range gate, at ground range $\tilde{r}_0 + \Delta_{\tilde{r}}/2$. Points E, F, and G lie along a line defined by the left edge of the azimuthal mainlobe, with azimuthal separation β_a from scene center point O; similarly, points H, I, and J lie along a line defined by the right edge of the azimuthal mainlobe, also with azimuthal separation β_a from scene center point O. For almost any $0° \leq \psi \leq 90°$, point G will achieve the maximum relative range rate with respect to point O, and point H will achieve the minimum relative range rate with respect to point O.[5] We can thus derive expressions for the MDV in the arbitrary imaging geometry by determining the range rates at points G and H.

[4]This will ultimately yield a result for MDV that can be trivially extended to values of ψ between 90° and 360°.

[5]For some ψ near 90°, point J may actually attain a relative range rate slightly more negative than that of point G, but the difference will be negligible for any reasonable θ and β_a. As such, the ensuing derivation concentrates on point G as the basis for MDV in an arbitrary imaging geometry.

Consider a right-handed coordinate system centered at the ground-projected location of the platform, as depicted in Figure 4. This coordinate system has z-axis oriented in the upward ground-normal direction, and y-axis oriented in the direction of platform velocity. In this coordinate system, the platform position is given by

$$\mathbf{P} = \begin{bmatrix} 0 \\ 0 \\ h \end{bmatrix} \tag{21}$$

and the scene center O has a position of

$$\mathbf{O} = \begin{bmatrix} \tilde{r}_0 \sin\psi \\ \tilde{r}_0 \cos\psi \\ 0 \end{bmatrix}. \tag{22}$$

It can be shown that point F is located at position

$$\mathbf{F} = \begin{bmatrix} -r_0 \cos\psi \tan\left(\frac{\beta_a}{2}\right) + \tilde{r}_0 \sin\psi \\ r_0 \sin\psi \tan\left(\frac{\beta_a}{2}\right) + \tilde{r}_0 \cos\psi \\ 0 \end{bmatrix} \tag{23}$$

and point I is located at position

$$\mathbf{I} = \begin{bmatrix} r_0 \cos\psi \tan\left(\frac{\beta_a}{2}\right) + \tilde{r}_0 \sin\psi \\ -r_0 \sin\psi \tan\left(\frac{\beta_a}{2}\right) + \tilde{r}_0 \cos\psi \\ 0 \end{bmatrix}. \tag{24}$$

It then follows that point G has a position of

$$\mathbf{G} = \mathbf{F}\left(1 + \frac{\Delta_{\tilde{r}}}{2\tilde{r}_0}\right) \tag{25}$$

and point H has a position of

$$\mathbf{H} = \mathbf{I}\left(1 - \frac{\Delta_{\tilde{r}}}{2\tilde{r}_0}\right). \tag{26}$$

The absolute range rate of point G can then be shown to be

$$\frac{dr_G}{dt} = v\frac{\left(\frac{1}{\cos\theta}\sin\psi\sin\frac{\beta_a}{2} + \cos\psi\cos\frac{\beta_a}{2}\right)\left(\tilde{r}_0 + \frac{\Delta_{\tilde{r}}}{2}\right)}{\left(\left(\tilde{r}_0 + \frac{\Delta_{\tilde{r}}}{2}\right)^2 + \left(h\cos\frac{\beta_a}{2}\right)^2\right)^{1/2}}. \tag{27}$$

Similarly, the absolute range rate of point H can be shown to be

$$\frac{dr_H}{dt} = v\frac{\left(\frac{1}{\cos\theta}\sin\psi\sin\frac{\beta_a}{2} + \cos\psi\cos\frac{\beta_a}{2}\right)\left(\tilde{r}_0 - \frac{\Delta_{\tilde{r}}}{2}\right)}{\left(\left(\tilde{r}_0 - \frac{\Delta_{\tilde{r}}}{2}\right)^2 + \left(h\cos\frac{\beta_a}{2}\right)^2\right)^{1/2}}. \tag{28}$$

The absolute range rate of the scene center is given by (5). For reasonable imaging geometries, the absolute difference between (27) and (5) will exceed the absolute difference between (28) and (5), and thus the MDV for an arbitrary imaging geometry is

$$\mathrm{MDV} = v \left[\frac{\left(\frac{1}{\cos\theta} \sin\psi \sin\frac{\beta_a}{2} + \cos\psi \cos\frac{\beta_a}{2} \right) \left(\tilde{r}_0 + \frac{\Delta_{\tilde{r}}}{2} \right)}{\left(\left(\tilde{r}_0 + \frac{\Delta_{\tilde{r}}}{2} \right)^2 + \left(h \cos\frac{\beta_a}{2} \right)^2 \right)^{1/2}} - \cos\theta \cos\psi \right]. \tag{29}$$

Note that this equation reduces approximately to (10) when $\psi = 90°$, and approximately to (19) when $\psi = 0°$.[6] Note also that while (29) holds only for $0° \leq \psi \leq 90°$, it can be trivially extended to hold for all other ψ. In particular, extension to $90° < \psi \leq 180°$ simply requires replacing ψ with $(180° - \psi)$; extension to $180° < \psi \leq 270°$ simply requires replacing ψ with $(\psi - 180°)$; extension to $270° < \psi < 360°$ simply requires changing the sign of ψ.

[6]The small discrepancies between (29) and the special-case equations of (10) and (19) for the appropriate values of ψ are attributable to the annular character of the range-gated projected mainlobe, which was taken into account in the current section but was neglected in Sections 2 and 3.

5 Summary and Caveats

This document has demonstrated the dependence of MDV on imaging geometry, antenna characteristics, and platform velocity. A general expression for MDV in an arbitrary imaging geometry is provided by (29). In the special case of broadside imaging, this expression reduces approximately to (10); in the special case of forward-looking imaging, this expression reduces approximately to (19). Although comparison of these three equations reveals significant differences in the detailed dependence of MDV on other parameters, they share an important fundamental similarity: regardless of imaging geometry, MDV is directly proportional to platform velocity. As such, the most practical path to a smaller MDV in any operational scenario is usually a reduction in platform velocity. This is especially true considering the various operational and physical limitations that underlie the other terms in the MDV equations.

One important consideration not explicitly apparent from the MDV equations is the difference in the direction of radial velocity inherent in each imaging geometry. In particular, because the radial velocity direction is defined by the look direction, different absolute directions of target motion will be inherently more or less detectable depending on the particular imaging geometry. Any selection of imaging geometry for an operational scenario must thus include not only a consideration of the MDV as in (29), but also a consideration of the prevalence or importance of different orientations of target motion. For example, consider a scenario in which it is known in advance that all target motion of interest will be oriented in a broadside direction relative to the platform velocity.[7] Even though a broadside imaging geometry will generally result in a much larger MDV than a forward-looking geometry, use of a broadside imaging mode in this scenario might be inherently desirable because a forward-looking scenario would result in a near-zero radial velocity for almost all object trajectories of interest.

The analysis presented in this document, although relatively realistic and representative, is subject to numerous caveats. First of all, it assumes that the range-gated ground projection of the antenna mainlobe is a clearly defined annular sector; in actuality, a radar beam is not defined by crisp boundaries but instead by rolloff in all directions. In addition, this analysis assumes that the range gate is symmetric about the scene center, which may or may not be the case for a particular sensor in a particular imaging mode. Furthermore, the analysis presented here neglects the impact of sidelobes or backlobes on the radar returns and the formed image. Finally, this analysis ignores the effect of target reflectivity on detectability: a bright target may in fact be easily detectable even with a radial velocity below MDV, depending on the intensity of the endoclutter and the chosen target detection algorithm.[8] In any particular scenario, one or all of the assumptions made here may not be strictly valid. For most applications, however, the analysis presented here is likely applicable.

[7] This might be the case in a border-patrol application, in which the platform might travel parallel to a linear border while surveilling the border for objects moving orthogonally across it.

[8] More generally, the basic concept of antenna beamwidth used here could be expanded to represent the beam positions at which the endoclutter exceeds particular fixed amplitudes, and thus the beam positions at which specific fixed-amplitude targets are equal in intensity to the endoclutter.

References

[1] A. W. Doerry. Performance limits for exo-clutter ground moving target inidicator (GMTI) radar. Technical Report SAND2010-5844, Sandia National Laboratories, Albuquerque, NM, September 2010.

[2] D. C. Schleher. *MTI and Pulsed Doppler Radar*. Artech House, Norwood, MA, 1991.

[3] R. J. Sullivan. *Microwave Radar: Imaging and Advanced Concepts*. Artech House, Norwood, MA, 2000.

DISTRIBUTION:

1	MS 1163	W. J. Bow, Jr., 5448
1	MS 1163	B. K. Bray, 5448
5	MS 1163	J. A. Richards, 5448
1	MS 1207	I. A. Erteza, 5962
1	MS 0899	Technical Library, 9536 (electronic copy)

v1.36

Sandia National Laboratories